Nonlocal Decoding of Positional and Correlational Information during Development

Alex Chen Yi Zhang,[1,*] Pablo Mateu Hoyos,[1] David Brückner,[2,†] and Gašper Tkačik[1,‡]
[1]Institute of Science and Technology Austria, Klosterneuburg AT-3400, Austria
[2]Biozentrum and Department of Physics, University of Basel, Basel CH-4056, Switzerland

(Received 16 January 2026; accepted 12 June 2026; published 15 July 2026)

In many developmental systems, cells differentiate into a tissue by reading out morphogen concentration fields, a process fundamentally limited by noise. How much can the precision of this process be improved by nonlocal information, e.g., via cell-cell communication? Using a Bayes-optimal framework, we show that positional inference depends crucially on morphogen spatial correlations and on the "structural prior" that encodes the geometry of the cellular lattice performing the readout, thereby determining what a cell can reliably assume about the position of its neighbors when interpreting nonlocal morphogen signals. We derive upper bounds on positional information gain due to nonlocal readout and identify signal processing algorithms that approximate optimal positional inference, as well as simple chemical reaction schemes which implement such algorithms. Our theory suggests that correlational information can be exploited to significantly enhance developmental precision.

DOI: 10.1103/mbjk-v4ym

During development, genetically identical cells reproducibly differentiate into distinct cell fates arranged in precise spatial patterns. In many systems, this patterning relies on positional information [1–3], a chemical "global positioning system" in which cells locally interpret graded morphogen concentration profiles to determine their positions within an embryo. The precision of this process is limited by intrinsic molecular noise that affects the morphogen readout in each cell independently, as well as by extrinsic—environmental or embryo-to-embryo—variability, which induces spatially correlated fluctuations in the morphogen signal. [4–7].

The concept of positional information has been formalized in information-theoretic terms as the mutual information, $\mathrm{PI} = I(X;G)$, between *position* x and a (possibly multidimensional) *morphogen value* g [8–10]. The higher the PI, the more accurately local morphogen levels can be mapped to positions along an embryonic or tissue axis.

A complementary view stipulates that the cells perform "decoding," or a statistical inference, of positions from the local morphogen concentrations [11,12]. If decoding is nearly Bayes-optimal (as suggested empirically [13,14]), position could be computed as a maximum *a posteriori* estimate $\hat{x} = \mathrm{argmax}_{x^*} P(x^*|g)$, and the mutual information between true and inferred positions provides, in practice, a tight approximation to positional information $\mathrm{PI} \simeq I(X,\hat{X})$ [15–17]. This relationship connects the encoding and decoding views of PI.

Both views assume that cells make independent inferences about their own position by relying only on local morphogen readouts. This is equivalent to neglecting spatially correlated fluctuations in the morphogen signal, which can be strong under dominant extrinsic noise. The assumption also precludes strategies where a cell could access nonlocal morphogen readouts, for instance via cell-cell communication or diffusion-mediated averaging [18–20]. Yet, experimental evidence suggests that nonlocal interactions can refine PI in several systems [21], e.g., the interpretation of the Wingless gradient in *Drosophila* wing discs [22]. More recently, the analyses of the anterior-posterior patterning in the fruit fly *Drosophila* demonstrate that information beyond local PI can be contained in, and extracted from, the spatial correlations in morphogen fluctuations [Fig. 1(a)] [5,23]. This possibility was theoretically foreshadowed by the extension of the positional information formalism to self-organized patterning [24], which identified correlational information (CI) as a measure of the additional information content of morphogen profiles due to spatial correlations in their fluctuations. Thus, even while morphogen profile ensembles with identical mean and local noise variance share the same PI, they can differ in their CI [Fig. 1(b)].

Here, we develop a mathematical framework to quantify the amount of information useful for patterning contained in spatial correlations of the morphogen signal, and to predict how this information can be optimally exploited through a formal treatment of nonlocal decoding. We organize our results using Marr's three levels of analysis of information

*Contact author: alexchenyi.zhang@ist.ac.at
†Contact author: d.b.brueckner@unibas.ch
‡Contact author: gtkacik@ist.ac.at

Published by the American Physical Society under the terms of the Creative Commons Attribution 4.0 International license. Further distribution of this work must maintain attribution to the author(s) and the published article's title, journal citation, and DOI.

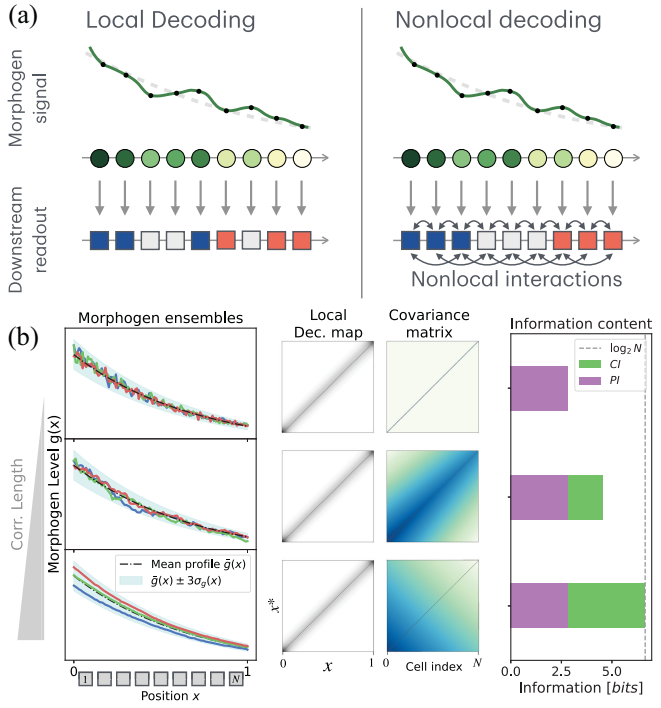


FIG. 1. (a) Cells arranged into a 1D lattice (squares; here and throughout $N = 100$ cells) read out a local, noisy morphogen signal (circles with different shades of green) to infer their positions and commit to corresponding cell fates (blue, white, and red squares). Signal noise can result in imprecise fate assignments (left), which could be mitigated by information exchange between cells, e.g., via diffusion-mediated averaging or other cell-cell coupling mechanisms (right). (b) Example morphogen ensembles (first column; color lines = individual profiles; black = mean) carrying the same PI and thus having identical local decoding maps (second column) [14], but differing in the spatial correlation structure (third column–see Sec. S2.A in [25] for details) and therefore in the amount of correlational information, CI (fourth column; dashed vertical line at $I = \log_2(N) \approx 6.6$ bits = perfect specification of every cell in the lattice).

processing systems, a paradigm well established in computational neuroscience [29], and recently extended to developmental patterning [30]: we first formally state the computational problem that the cells should be solving (Level I); next, we propose signal processing algorithms that approximate optimal solutions to this computational problem (Level II); finally, we provide a proof-of-principle, minimal biochemical network that can implement such algorithms (Level III).

Level I: Formalizing the problem—At the first level, our goal is to quantify the maximal gain in positional information achievable when a cell incorporates nonlocal morphogen readouts, and to determine how these gains depend on the statistical structure of the morphogen ensemble [Fig. 1(b)]. In contrast to local decoding, where a cell i relies only on its own readout g_i, nonlocal decoding allows inference based on morphogen readouts $\mathbf{g}$ taken at all cellular locations $\mathbf{x} = (x_1, \ldots, x_N)$. For the cell i, this amounts to $\hat{x}_i = \mathrm{argmax}_{x_i^*} P(x_i^*|\mathbf{g})$; if a cell only had access to information from a limited neighborhood $\mathcal{N}_i$, the posterior is correspondingly conditioned on $\{g_j\}_{j\in\mathcal{N}_i}$.

In general, the posterior can be written as

$$P(x_i^*|\mathbf{g}) \propto P(x_i^*) \int \mathrm{d}\mathbf{x}_{\neg i}^* P(\mathbf{g}|\mathbf{x}^*) P(\mathbf{x}_{\neg i}^*|x_i^*), \tag{1}$$

where $\mathbf{x}_{\neg i}^*$ denotes the vector of implied positions of all cells other than i. Thus, two key factors determine the limits to nonlocal positional decoding: (i) the correlation structure of morphogen fluctuations encoded in the likelihood $P(\mathbf{g}|\mathbf{x}^*)$; and (ii), the "structural prior," $P(\mathbf{x}_{\neg i}^*|x_i^*)$, which formalizes assumptions about the geometry and reproducibility of the cellular lattice. This prior is not merely a technical ingredient: it captures what cells can reliably assume about the positions of the neighbors, and in principle can be inferred empirically from measured cell positions across embryos. We formalize this prior through two complementary idealized limits—the relative location prior (RLP) and the absolute location prior (ALP)—introduced below.

Exact evaluation of Eq. (1) is generally intractable. To make analytical progress, we therefore focus on two idealized but informative limits of the structural priors, which define upper bounds on nonlocal decoding performance. For each case, we compute the mutual information between the true and inferred positions, $I(X, \hat{X}_{\mathrm{nl}})$, and compare it to the local decoding baseline, $I(X, \hat{X}_1)$. In the small noise regime with unimodal posteriors (see *Defining positional error* in [15]), positional information can be expressed as

$$\mathrm{PI} \simeq I(X, \hat{X}) \simeq -\left\langle \log_2 \frac{\sqrt{2\pi e \sigma_x^2(x)}}{L} \right\rangle_x, \tag{2}$$

where $\langle \cdots \rangle_x$ indicates averaging over spatial positions, L is the embryo length and the positional error, $\sigma_x^2(x) = \langle (x - x^*)^2 \rangle_{P(x^*|x)}$, is the mean squared inference error at position x, as visualized by the "decoding map" $P(x^*|x)$ [Fig. 1(b)] [14]. We define the information gain from nonlocal decoding as

$$\Delta\mathrm{PI} := I(X, \hat{X}_{\mathrm{nl}}) - I(X, \hat{X}_1). \tag{3}$$

Throughout, we assume that nonlocal morphogen readouts are communicated in an error-free fashion, without additional noise [31], allowing us to compute optimal bounds.

We first consider the RLP (Fig. 2), where cell i decodes the morphogen relying on the perfect knowledge about the relative positions $d_{ij} = x_j - x_i$ of its neighbors from which nonlocal morphogen readouts are received. The corresponding structural prior is

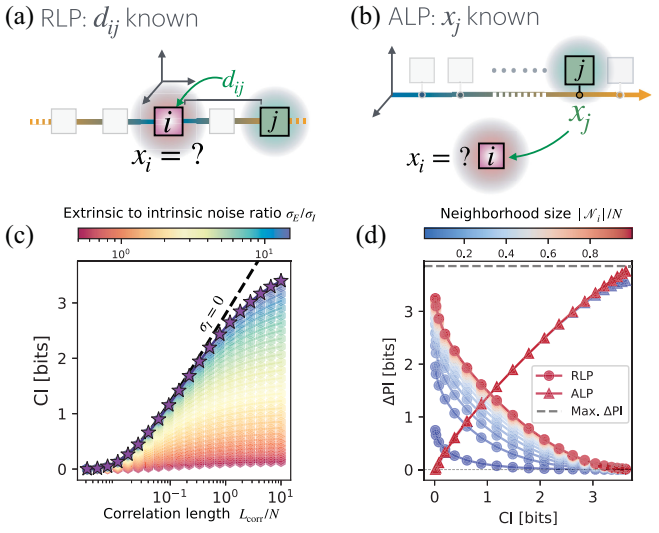


FIG. 2. A focal cell i (pink square) improves its positional inference with nonlocal morphogen information g_j read out by neighboring cells $j \in \mathcal{N}_i$. (a) For RLP, the nonlocal signal is interpreted in the context of perfectly known relative location, d_{ij}, of each "sender cell" (green square) that conveys the nonlocal signal. In reality, the relative distances would be imperfectly known (illustrated by blur). (b) For ALP, absolute locations, x_j, of sender cells are assumed known. In reality, the absolute locations would be imperfectly known. (c) Correlational information (CI) in the morphogen ensemble increases with the correlation length of the Gaussian fluctuations, L_{corr}, and their magnitude σ_E relative to the intrinsic (uncorrelated) noise with magnitude σ_I (colorbar). (d) Maximal PI increase with nonlocal decoding using RLP (circles) or ALP (triangles). Color indicates the neighborhood size $|\mathcal{N}_i|$ (dark blue: ± 1 nearest neighbor; dark red: entire system of N cells). Here and for the rest of the Letter, we consider $\sigma_E/\sigma_I = 15$ [violet stars in (c); see SM Fig. S1 for other σ_E/σ_I]. Dashed black line: ΔPI corresponding to perfect cellular specification.

$$P_{\mathrm{RLP}}(\mathbf{x}^*_{\neg i}|x^*_i) = \prod_{j\in\mathcal{N}_i} \delta[x^*_j - (x^*_i + d_{ij})]. \tag{4}$$

Under this assumption, the positional error of nonlocal decoding is (see SM [25] Sec. II.C):

$$\sigma^2_{x,\mathrm{RLP}}(x_i) \simeq \left(\sum\nolimits_{j,k\in\mathcal{N}_i} \bar{g}'(x_j)[C^{-1}_{\mathcal{N}_i}]_{jk}\bar{g}'(x_k)\right)^{-1}, \tag{5}$$

where $\bar{g}'(x)$ is the spatial derivative of the mean profile, and $C_{\mathcal{N}_i}$ is the covariance matrix of morphogen fluctuations restricted to the neighborhood $\mathcal{N}_i$. This expression generalizes the familiar result for local decoding from a single, $\sigma^2_x(x_i) \simeq (\bar{g}'(x_i)^2/C_{ii})^{-1}$, and from multiple gradients [14,15]; recently, it has been applied to data in the spatial context by analogy to the established result for the multigradient case [23].

To evaluate ΔPI, we generate morphogen ensembles with identical PI but different CI by varying the relative amplitude (σ_I/σ_E) and the correlation length (L_{corr}/N) of intrinsic (uncorrelated) and extrinsic (correlated) fluctuations [Fig. 2(c)]. For RLP decoding, the information gain ΔPI increases with the neighborhood size $|\mathcal{N}_i|$, and is largest when morphogen fluctuations are uncorrelated (i.e., at low CI) [Fig. 2(d)], while remaining substantial across a broad range of L_{corr} (SM Fig. S1).

We next consider the ALP, in which cell i is assumed to know the true positions, x_j, of its neighbors, so that

$$P_{\mathrm{ALP}}(\mathbf{x}^*_{\neg i}|x^*_i) = P(\mathbf{x}^*_{\neg i}) = \prod_{j\in\mathcal{N}_i} \delta(x^*_j - x_j). \tag{6}$$

In this case, the positional errors read

$$\sigma^2_{x,\mathrm{ALP}}(x_i) \simeq \left(\bar{g}'(x_i)^2[C^{-1}_{\mathcal{N}_i}]_{ii}\right)^{-1}, \tag{7}$$

leading to a compact expression for ΔPI (see SM [25] Sec. S2B):

$$\Delta\mathrm{PI}_{\mathrm{ALP}} = \frac{1}{2N}\sum_{i=1}^{N}[\log_2[C_{\mathcal{N}_i}]_{ii} + \log_2[C^{-1}_{\mathcal{N}_i}]_{ii}]. \tag{8}$$

Unlike RLP decoding, ALP decoding benefits from strong spatial correlations, with ΔPI increasing as morphogen fluctuations become more correlated [Fig. 2(d)]. We provide a clearer intuition for this behavior later in the text.

The RLP and ALP thus define complementary idealized limits, each corresponding to perfect knowledge of some aspect of the cellular lattice geometry. Real developmental systems are unlikely to satisfy either assumption exactly; nevertheless, these limits provide informative bounds that clarify how morphogen correlations and structural priors *jointly* shape the potential gains from nonlocal decoding. In the following section, we show that these bounds inform plausible algorithms that can approximate positional decoding, also in more realistic situations.

Level II: Algorithmic approximations—While the bounds in Eqs. (5) and (7) quantify the maximal gain achievable by nonlocal decoding, they do not specify how biological systems might algorithmically approximate such inference, which we study next. Guided by the contrasting behaviors of RLP and ALP decoding (Fig. 2), we focus on two limiting cases, one for RLP and one for ALP, so as to extract the representative algorithmic strategies.

We first consider RLP in the limit of uncorrelated morphogen fluctuations. As $L_{\mathrm{corr}} \to 0$, optimal *nonlocal* RLP decoding reduces to *local* decoding from an effective readout $g^{\mathrm{eff}}_i \propto \sum_{j\in\mathcal{N}_i} g_j$, i.e., a uniform pooling of morphogen signals over a local neighborhood (see SM Sec. S3A [25]). This suggests a simple algorithmic strategy in which morphogen profiles are first spatially smoothed and then decoded locally (Fig. 3).

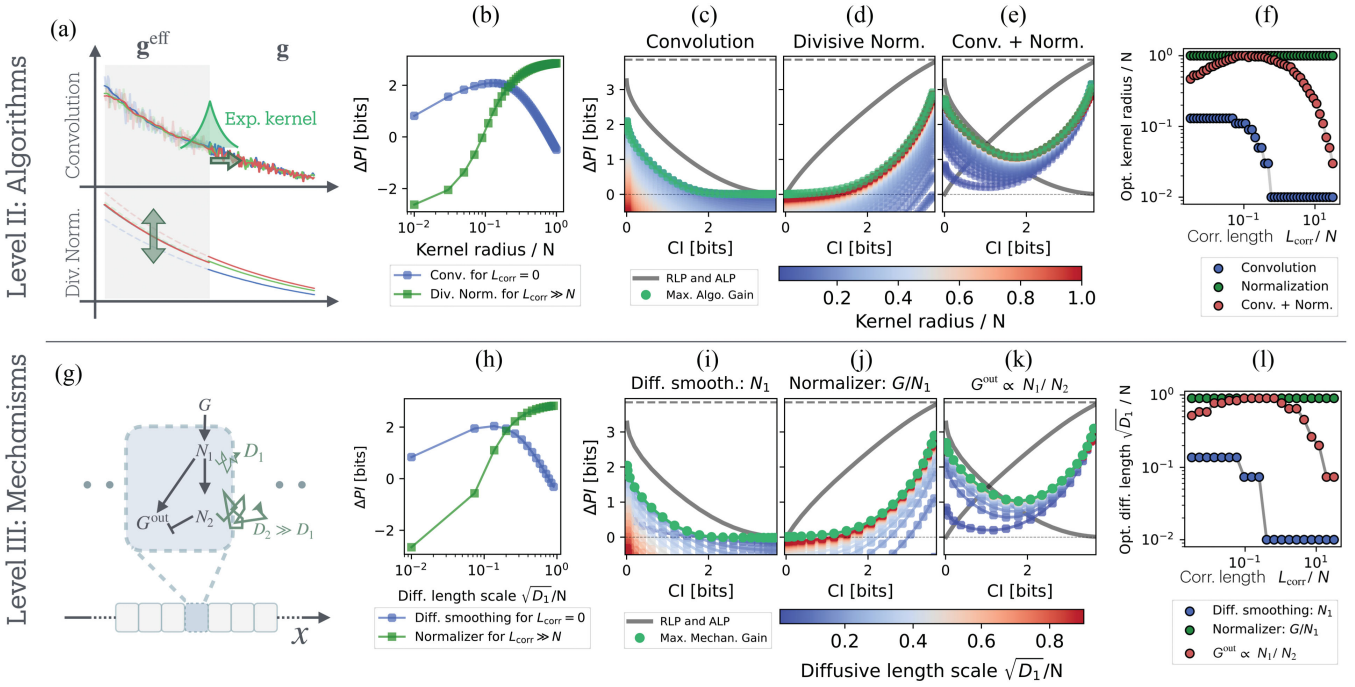


FIG. 3. (a) Algorithmic transformations map morphogen profiles $\mathbf{g}$ into effective profiles $\mathbf{g}^{\text{eff}}$ via spatial convolution and/or divisive normalization, which are subsequently decoded locally. (b) Information gain ΔPI for convolution and divisive normalization in the $L_{\text{corr}} = 0$ and $L_{\text{corr}} \gg N$ limits, respectively. ΔPI achieved by (c) convolution with exponential kernels of varying radii, across a range of CI values; (d) divisive normalization with a normalization constant obtained via convolution with kernels of varying radii; (e) sequential application of convolution (variable radius) and global normalization (sum over all N cells). (f) For each correlation length L_{corr}, the optimal kernel radius differs across the three algorithmic strategies. (g) Minimal reaction-diffusion circuit with two diffusible *normalizer* species (N_1, N_2) implements algorithmic operations of (a)–(f). (h)–(k) Same analyses as in (b)–(e), but using the reaction-diffusion implementation. (i) ΔPI associated with the steady-state profile N_1 while varying its diffusion length $\sqrt{D_1}/N$. (j) ΔPI associated with G/N_1 while varying $\sqrt{D_1}/N$. (k) ΔPI associated with N_1/N_1 while varying $\sqrt{D_1}/N$, with $\sqrt{D_2}/N$ fixed at $\approx 2.23 \gg \sqrt{D_1}/N$. (l) Optimal diffusion length scales with correlation length of morphogen fluctuations.

To evaluate the performance of such pooling strategies, we implement spatial convolution with kernels of varying shape and "radius" [Fig. 3(a)]. Across kernel choices, we find that positional information gain ΔPI is maximized at an intermediate kernel radius, remaining below but close to the optimal RLP bound [Fig. 3(b)]. Importantly, convolutional pooling yields substantial information gain not only in the strictly uncorrelated limit, but across a broad range of correlation lengths [Fig. 3(c)], provided the kernel radius is matched to the spatial scale of morphogen fluctuations [Fig. 3(f)]. The precise kernel shape only has minor effects (see SM Fig. S3 [25]).

We also explore more general optimal linear operators $\mathbf{L}$, $\mathbf{g}^{\text{eff}} = \mathbf{L}\mathbf{g}$, not restricted to having a convolutional form, which maximize positional information (SM Fig. S4 and Sec. S3C [25]). While too complex to inform mechanistic implementations, they provide an existence proof that the optimality bound can be reached with simple linear algorithms, as the theory predicts.

In contrast, ALP decoding benefits mostly from long-range correlated morphogen fluctuations [Fig. 3(c)]. In the $L_{\text{corr}} \to \infty$ limit—and assuming that the fluctuation magnitude scales with the mean morphogen levels, $\sigma^2_{i,E} \propto g_i^2$, as expected from purely extrinsic noise [7] in canonical source-diffusion-degradation models for morphogen gradient establishment [32]—the ALP decoding reduces to local decoding from a *nonlinear* effective readout $g_i^{\text{eff}} \propto g_i/G$, with $G = \sum_j g_j$, corresponding to divisive normalization of each profile by the global mean (see SM Sec. S3B [25]). Accordingly, the optimal kernel radius for this operation is the system size [Fig. 3(b), second panel]. Applying divisive normalization yields an information gain that increases with correlation length, qualitatively reproducing the behavior of the ALP bound [Fig. 3(d)]. This operation is closely related to divisive normalization in sensory neural systems [33], where it arises from efficient coding theory [34]. In our case, divisive normalization emerges as the optimal algorithmic approximation to Bayes-optimal ALP decoding in the fully correlated limit.

Sequential combinations: Unlike optimal bounds, which depend on specific assumptions about the structural prior, algorithmic approximations are operations that can be applied sequentially, e.g., convolutional smoothing

followed by divisive normalization. The resulting information gain shows a distinct nonmonotonic dependence on CI, with reduced gain at intermediate correlation length scales that are far from either limiting regime [Fig. 3(e)]. Nevertheless, the combined strategy consistently outperforms either algorithm applied in isolation, and over a broad range of CI, yields synergistic gains exceeding the sum of individual contributions. Such sequential transformations are reminiscent of multilayered biological networks that are thought to "refine" the positional information [9,30].

Level III: Mechanistic implementations—Finally, we ask whether the algorithmic operations identified above can be implemented by simple biochemical mechanisms. We consider a simple proof-of-concept reaction-diffusion biochemical network [Fig. 3(g)], that operates on a static input morphogen profile and transforms it into a refined output profile, $g^{\text{out}}(x,t)$, by filtering out much of the short- and long-range fluctuations in the input signal with the help of two intermediary diffusible *normalizer* chemical species n_1 and n_2 [24]. In this reaction scheme, g^{out} can be seen as a Level III realization of the "effective" signal g^{eff} discussed previously, which can be *locally* decoded into precise positional estimates.

We consider the following reaction-diffusion system:

$$\frac{\partial n_1}{\partial t} = D_1 \nabla^2 n_1 + \alpha_1 g - \kappa_1 n_1 \tag{9}$$

$$\frac{\partial n_2}{\partial t} = D_2 \nabla^2 n_2 + \alpha_2 n_1 - \kappa_2 n_2 \tag{10}$$

$$\frac{dg^{\text{out}}}{dt} = \alpha^{\text{out}} n_1 - \kappa^{\text{out}} n_2 g^{\text{out}}, \tag{11}$$

with $D_2 \gg D_1$ (see SM [25] Sec. S4).

At steady state, the input morphogen profile g is filtered into n_1, which naturally acts as its spatially smoothed version; therefore, the first equation describes a mechanism implementing convolution. The fast-diffusing species n_2 serves as a global integrator, which can be used to normalize extrinsic fluctuations via an n_2-dependent degradation rate of g^{out} in Eq. (11). The final output g^{out} is thus proportional to n_1/n_2 at steady state, thereby performing convolution followed by divisive normalization. As shown in Figs. 3(h)–3(l), this minimal circuit reproduces the ΔPI obtained from the algorithmic approximations with a surprising degree of quantitative agreement.

Several known signaling systems instantiate the key mechanistic ingredients of the chemical reaction circuit we considered. Differential diffusivity of Lefty and Nodal in zebrafish [35], combined with the Lefty-mediated inhibition of Smad2 phosphorylation, would be consistent with our proposal. Similar circuits, implicated in gradient scaling [36–38], could additionally contribute to patterning precision in line with our suggestions, with perturbations of N_1 and N_2 predicted to differentially affect within- versus across-embryo variability in cell fate specification. More generally, the reaction circuit we considered here is a proof-of-principle; other mechanisms generating long-range interactions mimicking the role of N_2 (e.g., mechanical gradients [39–41]) could subserve the necessary algorithmic roles for our proposed scheme.

Conclusions—A large body of theoretical and experimental work has investigated the limits of reproducibility in cell fate patterns driven by morphogen gradients [2–4]. While such patterning is often viewed as a cell-autonomous, local, single-step process of morphogen interpretation [2,3], patterning precision could be "refined" across consecutive steps [9,30,42], when cells are allowed to communicate [21].

Here, we formalize the problem of refining positional information through spatial information exchange, which could be mediated by very diverse cell-cell coupling mechanisms. We show that (i) optimal nonlocal decoding can substantially increase positional information in a manner dependent on the CI present in the morphogen ensemble; (ii) nonlocal decoding can be approximated by a combination of simple algorithmic transformations across a wide range of morphogen ensembles with different fluctuation correlation structures; (iii) such algorithmic transformations can be realized by simple reaction-diffusion-based biochemical networks. Taken together, our results demonstrate that the information-theoretic gains of nonlocal decoding are not solely a theoretical curiosity, but could be approached by biological systems. Furthermore, our results provide a framework within which we can attempt to rationalize and interpret the observed multilayered developmental regulatory cascades [30].

Our results highlight an important dichotomy: with RLP, correlations are detrimental because they make the information pooled by neighbors redundant. In contrast, with ALPs, correlations are beneficial because they reduce the effective number of degrees of freedom in the morphogen ensemble, and thus provide a useful collective signal about the fluctuation that can be utilized to "undo" its confounding effect. These qualitative differences in optimal signal processing due to different noise and prior statistics are reminiscent of results in cell signaling [43] and in neuroscience [44]. Our results show that correlations are not intrinsically good or bad: their utility for reproducible patterning depends on the structural prior about the neighbors that cells might have evolved to rely on in order to interpret nonlocal morphogen signal efficiently.

Taken together, our results emphasize that the cellular lattice—its geometry, reproducibility, and modes of cell-cell communication it supports—is as important as the morphogen gradients themselves in shaping positional information. Relaxing our idealized setting, by incorporating finite precision of cell positioning [45] and the constraints imposed by noisy information exchange between

cells [31,46], will be an important step towards assessing how closely biological systems can approach these theoretical limits.

Acknowledgments—This work was supported in part by European Research Council No. ERC-2023-SyG "DynaTrans" Grant No. 101118866 (G. T.). We thank Pieter Rein ten Wolde and Vahe Galstyan for stimulating discussions.

Data availability—Code to evaluate PI, to run algorithmic implementations of ALP and RLP decoding, and to perform simulations is publicly available at [47].

[1] L. Wolpert, Positional information and the spatial pattern of cellular differentiation, J. Theor. Biol. **25**, 1 (1969).
[2] K. W. Rogers and A. F. Schier, Morphogen gradients: From generation to interpretation, Annu. Rev. Cell Dev. Biol. **27**, 377 (2011).
[3] A. Kicheva and J. Briscoe, Control of tissue development by morphogens, Annu. Rev. Cell Dev. Biol. **39**, 91 (2023).
[4] T. Gregor, D. W. Tank, E. F. Wieschaus, and W. Bialek, Probing the limits to positional information, Cell **130**, 153 (2007).
[5] L. McGough, H. Casademunt, M. Nikolić, Z. Aridor, M. D. Petkova, T. Gregor, and W. Bialek, Finding the last bits of positional information, PRX Life **2**, 013016 (2024).
[6] M. B. Elowitz, A. J. Levine, E. D. Siggia, and P. S. Swain, Stochastic gene expression in a single cell, Science **297**, 1183 (2002).
[7] P. S. Swain, M. B. Elowitz, and E. D. Siggia, Intrinsic and extrinsic contributions to stochasticity in gene expression, Proc. Natl. Acad. Sci. U.S.A. **99**, 12795 (2002).
[8] J. O. Dubuis, G. Tkačik, E. F. Wieschaus, T. Gregor, and W. Bialek, Positional information, in bits, Proc. Natl. Acad. Sci. U.S.A. **110**, 16301 (2013).
[9] G. Tkačik and T. Gregor, The many bits of positional information, Development (Cambridge, U.K.) **148**, dev176065 (2021).
[10] M. Bauer, M. D. Petkova, T. Gregor, E. F. Wieschaus, and W. Bialek, Trading bits in the readout from a genetic network, Proc. Natl. Acad. Sci. U.S.A. **118**, e2109011118 (2021).
[11] K.-i. Hironaka and Y. Morishita, Encoding and decoding of positional information in morphogen-dependent patterning, Curr. Opin. Genet. Dev. **22**, 553 (2012).
[12] Y. Morishita and Y. Iwasa, Coding design of positional information for robust morphogenesis, Biophys. J. **101**, 2324 (2011).
[13] M. Zagorski, Y. Tabata, N. Brandenberg, M. P. Lutolf, G. Tkačik, T. Bollenbach, J. Briscoe, and A. Kicheva, Decoding of position in the developing neural tube from antiparallel morphogen gradients, Science **356**, 1379 (2017).
[14] M. D. Petkova, G. Tkačik, W. Bialek, E. F. Wieschaus, and T. Gregor, Optimal decoding of cellular identities in a genetic network, Cell **176**, 844 (2019).
[15] G. Tkačik, J. O. Dubuis, M. D. Petkova, and T. Gregor, Positional information, positional error, and readout precision in morphogenesis: A mathematical framework, Genetics **199**, 39 (2015).
[16] S. A. Cepeda-Humerez, J. Ruess, and G. Tkačik, Estimating information in time-varying signals, PLoS Comput. Biol. **15**, e1007290 (2019).
[17] M. Hledík, T. R. Sokolowski, and G. Tkačik, A tight upper bound on mutual information, in *2019 IEEE Information Theory Workshop (ITW)* (IEEE, New York, 2019), pp. 1–5.
[18] T. Erdmann, M. Howard, and P. R. Ten Wolde, Role of spatial averaging in the precision of gene expression patterns, Phys. Rev. Lett. **103**, 258101 (2009).
[19] P. Hillenbrand, U. Gerland, and G. Tkačik, Beyond the french flag model: exploiting spatial and gene regulatory interactions for positional information, PLoS One **11**, e0163628 (2016).
[20] T. R. Sokolowski and G. Tkačik, Optimizing information flow in small genetic networks. IV. Spatial coupling, Phys. Rev. E **91**, 062710 (2015).
[21] S. Herszterg, S. Cicolini, M. de Gennes, A. Huang, A. Matamoro-Vidal, C. Alexandre, M. Smith, H. Araujo, R. Levayer, J.-P. Vincent, and G. Salbreux, Signaling-dependent refinement of cell fate choice during tissue remodeling in *Drosophila* pupal wings, Dev. Cell **60**, 3480 (2025).
[22] E. Piddini and J.-P. Vincent, Interpretation of the wingless gradient requires signaling-induced self-inhibition, Cell **136**, 296 (2009).
[23] M. Erez, R. Friedman, and M. Nitzan, Neighborhood-informed positional information for precise cell identity specification, 10.1101/2025.03.17.643609 (2025).
[24] D. B. Brückner and G. Tkačik, Information content and optimization of self-organized developmental systems, Proc. Natl. Acad. Sci. U.S.A. **121**, e2322326121 (2024).
[25] See Supplemental Material at http://link.aps.org/supplemental/10.1103/mbjk-v4ym for additional theoretical and methodological details supporting the main text. The SM includes Refs. [26–28].
[26] T. M. Cover and J. A. Thomas, *Elements of Information Theory*, 2nd ed. (Wiley-Interscience, Hoboken, NJ, 2006).
[27] C. E. Rasmussen and C. K. I. Williams, *Gaussian Processes for Machine Learning* (MIT Press, Cambridge, MA, 2005).
[28] D. J. C. MacKay, *Information Theory, Inference, and Learning Algorithms*, 22nd ed. (Cambridge University Press, Cambridge, England, 2019).
[29] D. Marr and T. Poggio, From understanding computation to understanding neural circuitry, AI Memos (MIT), AIM Cambridge, MA, (1976).
[30] D. B. Brückner and G. Tkačik, Marr's three levels for embryonic development: Information dynamical systems, gene networks, PRX Life **4**, 017001 (2026).
[31] A. Mugler, A. Levchenko, and I. Nemenman, Limits to the precision of gradient sensing with spatial communication and temporal integration, Proc. Natl. Acad. Sci. U.S.A. **113**, E689 (2016).
[32] O. Grimm, M. Coppey, and E. Wieschaus, Modelling the bicoid gradient, Development (Cambridge, U.K.) **137**, 2253 (2010).
[33] M. Carandini and D. J. Heeger, Normalization as a canonical neural computation, Nat. Rev. Neurosci. **13**, 51 (2012).
[34] S. Lyu and E. P. Simoncelli, Nonlinear image representation using divisive normalization, in *2008 IEEE Conference on*

Computer Vision and Pattern Recognition (IEEE, New York, 2008), pp. 1–8.

[35] P. Müller, K. W. Rogers, B. M. Jordan, J. S. Lee, D. Robson, S. Ramanathan, and A. F. Schier, Differential diffusivity of nodal and lefty underlies a reaction-diffusion patterning system, Science **336**, 721 (2012).

[36] H. G. Othmer and E. Pate, Scale-invariance in reaction-diffusion models of spatial pattern formation, Proc. Natl. Acad. Sci. U.S.A. **77**, 4180 (1980).

[37] D. Ben-Zvi, B.-Z. Shilo, A. Fainsod, and N. Barkai, Scaling of the BMP activation gradient in Xenopus embryos, Nature (London) **453**, 1205 (2008).

[38] D. Ben-Zvi and N. Barkai, Scaling of morphogen gradients by an expansion-repression integral feedback control, Proc. Natl. Acad. Sci. U.S.A. **107**, 6924 (2010).

[39] A. Bailles, E. W. Gehrels, and T. Lecuit, Mechanochemical principles of spatial and temporal patterns in cells and tissues, Annu. Rev. Cell Dev. Biol. **38**, 321 (2022).

[40] C. Autorino, D. Khoromskaia, L. Harari, E. Floris, H. Booth, C. Pallares-Cartes, V. Petrasiunaite, M. Dorrity, B. Corominas-Murtra, Z. Hadjivasiliou, and N. I. Petridou, A closed feedback between tissue phase transitions and morphogen gradients drives patterning dynamics, (2025).

[41] C. Pérez-González, D. B. Brückner, M. Di-Luoffo, S. Richon, R. Goswami, M. Baghdadi, F. Piastra-Facon, N. Felsenthal, R. Bouras, A. Fumagalli, M. van der Net, M. Gloerich, S. Girardo, J. Guck, J. van Rheenen, J. Guillermet-Guibert, E. Hannezo, and D. M. Vignjevic, Self-organization of tumor heterogeneity and plasticity, 10.1101/2025.10.09.681487 (2025).

[42] A. Kicheva and J. Briscoe, Developmental pattern formation in phases, Trends Cell Biol. **25**, 579 (2015).

[43] J. Selimkhanov, B. Taylor, J. Yao, A. Pilko, J. Albeck, A. Hoffmann, L. Tsimring, and R. Wollman, Accurate information transmission through dynamic biochemical signaling networks, Science **346**, 1370 (2014).

[44] G. Tkačik, J. S. Prentice, V. Balasubramanian, and E. Schneidman, Optimal population coding by noisy spiking neurons, Proc. Natl. Acad. Sci. U.S.A. **107**, 14419 (2010).

[45] V. E. Deneke, A. Puliafito, D. Krueger, A. V. Narla, A. D. Simone, L. Primo, M. Vergassola, S. D. Renzis, and S. D. Talia, Self-organized nuclear positioning synchronizes the cell cycle in drosophila embryos, Cell **177**, 925 (2019).

[46] M. Majka, N. B. Becker, P. R. ten Wolde, M. Zagorski, and T. R. Sokolowski, Stable developmental patterns of gene expression without morphogen gradients, PLoS Comput. Biol. **20**, e1012555 (2024).

[47] https://github.com/alex-chenyi-zhang/nonlocdec_pici.